

Periodic event-triggered sampling and dual-rate control for a wireless networked control system with applications to UAVs

Citation for published version (APA):

Cuenca, A., Antunes, D., Castillo, A., Gil, G., Asadi Khashooei, B., & Heemels, W. P. M. H. (2019). Periodic event-triggered sampling and dual-rate control for a wireless networked control system with applications to UAVs. *IEEE Transactions on Industrial Electronics*, 66(4), 3157-3166. Article 8400587. <https://doi.org/10.1109/TIE.2018.2850018>

Document license:

TAVERNE

DOI:

[10.1109/TIE.2018.2850018](https://doi.org/10.1109/TIE.2018.2850018)

Document status and date:

Published: 01/04/2019

Document Version:

Publisher's PDF, also known as Version of Record (includes final page, issue and volume numbers)

Please check the document version of this publication:

- A submitted manuscript is the version of the article upon submission and before peer-review. There can be important differences between the submitted version and the official published version of record. People interested in the research are advised to contact the author for the final version of the publication, or visit the DOI to the publisher's website.
- The final author version and the galley proof are versions of the publication after peer review.
- The final published version features the final layout of the paper including the volume, issue and page numbers.

[Link to publication](#)

General rights

Copyright and moral rights for the publications made accessible in the public portal are retained by the authors and/or other copyright owners and it is a condition of accessing publications that users recognise and abide by the legal requirements associated with these rights.

- Users may download and print one copy of any publication from the public portal for the purpose of private study or research.
- You may not further distribute the material or use it for any profit-making activity or commercial gain
- You may freely distribute the URL identifying the publication in the public portal.

If the publication is distributed under the terms of Article 25fa of the Dutch Copyright Act, indicated by the "Taverne" license above, please follow below link for the End User Agreement:

www.tue.nl/taverne






Take down policy

If you believe that this document breaches copyright please contact us at:

openaccess@tue.nl

providing details and we will investigate your claim.

Periodic Event-Triggered Sampling and Dual-Rate Control for a Wireless Networked Control System With Applications to UAVs

Ángel Cuenca , Duarte J. Antunes , *Member, IEEE*, Alberto Castillo , *Student Member, IEEE*, Pedro García , Behnam Asadi Khashooei, and W. P. M. H. Heemels , *Fellow, IEEE*

Abstract—In this paper, periodic event-triggered sampling and dual-rate control techniques are integrated in a wireless networked control system (WNCS), where time-varying network-induced delays and packet disorder are present. Compared to the conventional time-triggered sampling paradigm, the control solution is able to considerably reduce network utilization (number of transmissions), while retaining a satisfactory control performance. Stability for the proposed WNCS is ensured using linear matrix inequalities. Simulation results show the main benefits of the control approach, which are experimentally validated by means of an unmanned-aerial-vehicle-based test-bed platform.

Index Terms—Event-triggered sampling, multirate control, networked control system, unmanned aerial vehicle (UAV).

I. INTRODUCTION

THE recent proposal of using event-triggered sampling (ETS), instead of time-triggered sampling (TTS), in control systems [1]–[3] has become a trending research area. While in the TTS strategy, the plant is periodically sampled, in the ETS approach, the plant is only sampled “when necessary,” that is, when state or output variables satisfy a certain event

Manuscript received January 7, 2018; revised May 2, 2018; accepted June 5, 2018. Date of publication June 29, 2018; date of current version November 30, 2018. This work was supported in part by the European Commission as part of Project H2020-SEC-2016-2017—Topic: SEC-20-BES-2016 (Id: 740736)—“C2 Advanced Multi-domain Environment and Live Observation Technologies,” in part by the European Regional Development Fund as part of OPZuid 2014-2020 under the Drone Safety Cluster project, in part by the Innovational Research Incentives Scheme under the VICI Grant “Wireless control systems: A new frontier in automation” (No. 11382) awarded by The Netherlands Organization for Scientific Research Applied and Engineering Sciences, and in part by the Ministerio de Economía y Competitividad, Spain, under Project FPU15/02008. (Corresponding author: Ángel Cuenca.)

Á. Cuenca, A. Castillo, and P. García are with the Instituto Universitario de Automática e Informática Industrial, Universitat Politècnica de València, 46022 Valencia, Spain (e-mail: acuenca@isa.upv.es; alcasfra@upvnet.upv.es; pggil@isa.upv.es).

D. J. Antunes, B. A. Khashooei, and W. P. M. H. Heemels are with the Control Systems Technology Group, Department of Mechanical Engineering, Eindhoven University of Technology, 5612 AZ Eindhoven, The Netherlands (e-mail: d.antunes@tue.nl; B.Asadi.Khashooei@tue.nl; m.heemels@tue.nl).

Color versions of one or more of the figures in this paper are available online at <http://ieeexplore.ieee.org>.

Digital Object Identifier 10.1109/TIE.2018.2850018

condition. In this way, ETS (compared to TTS) is better equipped to lead to a reduction of resource utilization. However, the ETS strategy manages less system information, and therefore, control performance may be worsened (compared to the desired one, which is defined by the TTS case) if the ETS schemes are not designed appropriately. In particular, model-based control techniques [4], [5] for the ETS strategy might be beneficial to guarantee a satisfactory control performance.

Integrating ideas from TTS and ETS paradigms results in periodic event-triggered sampling (PETS), where the event-triggering conditions are evaluated periodically. Different works on PETS can be found for linear systems (using, e.g., both state-feedback and output-feedback control solutions [3], [6], [7], observer-based control [4], multirate control [8], H_∞ control [9], and Youla–Kucera-like parameterization techniques [10]) and for nonlinear systems (using, e.g., state-feedback control [11], [12], output-feedback control [13], and observer-based control [14]). PETS can be studied either in a continuous-time framework (see, e.g., [15]) or in a discrete-time one (see, e.g., [16]). In the present work, the second perspective is adopted by means of a dual-rate controller, which is configured to update the control signal N times faster (at period T) than the sampling rate of the system’s output (at period NT). From the current measurement, the dual-rate controller is able to generate N control actions to be injected in the next N control periods. The sampling time T should be set to reach the required control performance from a single-rate framework. Actuating at this period T , and despite sensing at period NT , the dual-rate controller is able to preserve stability and keep a satisfactory control performance [17], [18]. One advantage of adopting dual-rate control in PETS is that the evaluation period of the triggering conditions can be enlarged, which leads to various implementation benefits, in addition to guaranteeing a minimum interevent time [15]. The main drawback of using dual-rate control (compared to single-rate control) is the consideration of more complex design techniques. In addition, the single-rate controller at period T may achieve better control performance.

Networked control systems (NCS) [19], [20] is a related prolific control area, addressing control scenarios where different devices share a common communication link. There are several advantages associated with NCS (such as cost reduction flexibility and ease of installation and maintenance), but also

drawbacks (like the possible occurrence of time-varying delays [21], [22], packet dropouts [23], [24], packet disorder [24], [25], and network bandwidth constraints [26], [27]).

The main aim of this work is twofold. First, the integration of PETS and dual-rate control in the context of wireless networked control systems (WNCS) in order to reduce the number of transmissions through the network (which may be related to the battery usage of the different wireless devices connected to the WNCS), while preserving stability and performance properties. For this purpose, it is essential to face the drawbacks considered in WNCS, that is, the presence of the following.

- 1) *Time-varying delays*: They can be compensated by means of the dual-rate controller by considering a gain-scheduling approach (for example, the one introduced in [28]). The control system becomes a discrete linear time-varying system, and its stability can be proved in terms of linear matrix inequalities (LMIs) [29].
- 2) *Packet disorders*: As the statistical distribution of the network-induced delay is assumed to be known, the sensing period can be chosen larger than the maximum time delay found in the delay distribution. Then, one can guarantee that no packet disorder will occur. In situations where the sensing period is long (say, in the same order as the settling time), dual-rate setups (i.e., actuating faster than sensing) may be advantageous in terms of achievable performance [17], [18].

Our second aim is to show the potential of our ideas in the context of a popular control application, that of unmanned aerial vehicles (UAVs). In fact, the large number of UAV applications has attracted the interest of the research community [30]–[32]. In order to autonomously navigate, an imperative need of UAVs is the ability to accurately position the UAV in the environment. Therefore, one of the main tasks in this research area is the design of position controllers, from conventional proportional–derivative (PD) controllers [33], [34] to more sophisticated ones [35]–[37]. In the present work, an advanced PD controller such as the proposed gain-scheduled dual-rate one will be used to wirelessly control the orientation on the z -axis of a UAV. The use of WNCS in UAV-based platforms enables to use less on-board hardware, and hence, the total weight of the platform can be significantly decreased. For instance, while vision, navigation, and control algorithms can be implemented on the onboard computer, optical flow computations, flight data monitoring, and trajectory generation can be performed on the ground control station (GCS) (e.g., [30]). Clearly, including PETS may be beneficial and even needed, since the energy usage of battery-powered devices and the utilization of communication resources can be reduced [4]. Demonstrators of PETS schemes are rare; exceptions are [38]–[41]. As such, the experimental validation, next to the novel design, is a contribution of its own. To the best of the authors' knowledge, only one very recent work [8] proposes a dual-rate PETS control solution in an NCS framework, where time-varying delays are dealt with. But in [8], no experimental validation is included. Other differences between [8] and the present work are: 1) the controller design framework (continuous-time and a Lyapunov–Krasovskii method are used

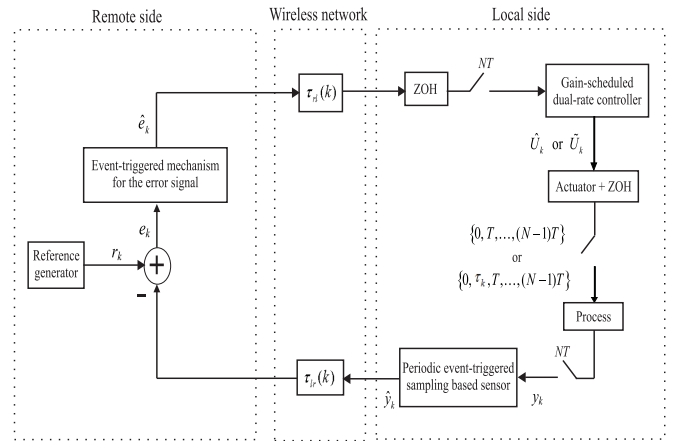


Fig. 1. NCS setup.

in [8], whereas discrete-time and a gain-scheduling approach are employed in our work); and 2) stability analysis (global asymptotic stability is guaranteed in [8], whereas mean square stability will be assessed in this work).

The rest of this paper is organized as follows. In Section II, the considered WNCS is described. Section III presents the stability analysis for the control system. In addition, some cost functions are included in order to be used when analyzing control performance and reduction of resource usage for the WNCS. Section IV presents a UAV-based platform, which enables to validate the control solution, after being simulated in Truetime [42]. Finally, Section V enumerates the main conclusions of the work.

II. PROBLEM SETTING

The considered networked setup is shown in Fig. 1. In the following subsections, its different features will be explained.

A. Process, Network-Induced Delay, and Dual-Rate Controller

Let us consider an n -order process, which is sampled using a dual-rate scheme considering the actuation rate $1/T$ and the sensing rate $1/NT$ (N is a given integer). It can be represented in a lifted framework [43] as

$$\begin{aligned} x_{k+1} &= A_P x_k + B_P U_k \\ y_k &= C_P x_k + D_P U_k \end{aligned} \quad (1)$$

where $x_k \in \mathbb{R}^n$ is the plant state vector ($k \in \mathbb{N}$ represents instants at period NT), y_k is the output measurement, and $U_k \in \mathbb{R}^N$, being $U_k = (u_1^k, u_2^k, \dots, u_N^k)^T$, is the control input sequence with $(\cdot)^T$ denoting transpose, where the actuation updates occur at evenly spaced instants $kNT + lT$ ($l = 0, 1, \dots, N-1$) under zero-order-hold (ZOH) conditions (i.e., u_1^k is applied at kNT , u_2^k is applied at $kNT + T$, and so on up to u_N^k , which is applied at $kNT + (N-1)T$). That leads to a uniform actuation pattern $\{0, T, \dots, (N-1)T\}$ inside the sensor period. Matrices in (1) are $A_P \in \mathbb{R}^{n \times n}$, $B_P \in \mathbb{R}^{n \times N}$,

$C_P \in \mathbb{R}^{1 \times n}$, and $D_P \in \mathbb{R}^{1 \times N}$. As usual in most of the physical systems, we will assume $D_P = 0$ in the following.

When the process is wirelessly controlled, network-induced delays usually appear. The discrete round-trip time delay $\tau_k \in \mathbb{R}_{\geq 0}$ is defined as

$$\tau_k := \tau_{rl}(k) + \tau_c(k) + \tau_{lr}(k) \quad (2)$$

where $\tau_{lr}(k)$ is the local-to-remote delay, $\tau_{rl}(k)$ is the remote-to-local delay, and $\tau_c(k)$ is a computation time delay required by the different devices, which is lumped together with the network-induced delays. As it will be shown later, the method employed in this work requires different mathematical operations, being matrix multiplication the most complex one and, hence, requiring the largest amount of computation time. When this operation is used in the present work, it concretely involves the multiplication of two matrices with dimensions $n \times m$ and $m \times 1$ (i.e., an array of m elements). The computation complexity is then $O(nm)$. The round-trip delay τ_k is assumed to be time-varying in the range $[0, \tau_{\max}]$, with $\tau_{\max} < NT$. This assumption prevents packet disorder. The local side is assumed to have computation capabilities in order to execute the gain-scheduling controller. As a local clock is governing the different local devices, they can be perfectly synchronized. Therefore, no additional synchronization and time-stamping techniques are required in order to measure the round-trip time delay. τ_k can be obtained by subtracting packet sending and receiving times. Once the delay is measured, the local gain-scheduling controller will compensate for it. The procedure works under the assumption of no packet disorder (as previously pointed out) and no packet dropouts. Note that, although a shared clock can be assumed in some applications (as in the present work), it might be hard to fulfill for other applications, for instance, in multiple wireless sensor nodes that are physically distributed. In this case, an option may be to synchronize nodes [44]. One of the main drawbacks of using synchronization (which is required by the time-stamping technique) arises when an accurate delay measurement is needed. In this case, the synchronization protocol may need to send a large quantity of special messages, increasing network load and hence delays. A probabilistic model for the network delays τ_k is considered. In fact, the τ_k are assumed to be independent and identically distributed random variables with a known probability function $p(\tau_k) : \mathbb{R}_{\geq 0} \rightarrow \mathbb{R}_{\geq 0}$. As will be shown later in Section IV, in our wireless Ethernet configuration, the probability function can be fitted to a generalized exponential distribution (such as in [45]).

The delay-dependent dual-rate controller, which is located at the local side, will take in the lifted framework the form

$$\begin{aligned} \phi_{k+1} &= A_R(\tau_k)\phi_k + B_R(\tau_k)\hat{e}_k \\ U_k &= C_R(\tau_k)\phi_k + D_R(\tau_k)\hat{e}_k \end{aligned} \quad (3)$$

where $\phi_k \in \mathbb{R}^2$ is the state vector, and \hat{e}_k is the error signal received by the controller (which will be defined in (9)). In this work, $A_R(\tau_k) \in \mathbb{R}^{2 \times 2}$, $B_R(\tau_k) \in \mathbb{R}^2$, $C_R(\tau_k) \in \mathbb{R}^{N \times 2}$, and

$D_R(\tau_k) \in \mathbb{R}^N$ represent a dual-rate PD controller, where

$$\begin{aligned} A_R(\tau_k) &= \begin{pmatrix} 1 & 0 \\ 0 & f(\tau_k) \end{pmatrix} \\ B_R(\tau_k) &= \begin{pmatrix} 0 \\ 1 - f(\tau_k) \end{pmatrix} \\ C_R(\tau_k) &= \begin{pmatrix} 1 & -K_d(\tau_k) \\ 1 & 0 \\ \vdots & \vdots \\ 1 & 0 \end{pmatrix} \\ D_R(\tau_k) &= \begin{pmatrix} K_p(\tau_k) + K_d(\tau_k) \\ K_p(\tau_k) \\ \vdots \\ K_p(\tau_k) \end{pmatrix} \end{aligned} \quad (4)$$

being $K_p(\tau_k)$, $K_d(\tau_k)$, and $f(\tau_k)$, respectively, the proportional and derivative gains and a derivative noise-filter pole. All of these controller parameters can be captured in the delay-dependent gain vector $\theta(\tau_k) = (K_p(\tau_k), K_d(\tau_k), f(\tau_k))^T$, which will be computed by means of the gain scheduling approach

$$\theta(\tau_k) = \theta(0) + \Omega \cdot \tau_k \quad (5)$$

where

- 1) $\theta(0) = (K_p(0), K_d(0), f(0))^T$ is the no-delay nominal gain vector, which can be designed via classical procedures [46], [47].
- 2) Ω denotes the scheduling vector, which is deduced after solving a least-squares problem on the minimization of the first-order Taylor term of $\|\pi(\tau_k, \theta(\tau_k)) - \pi(0, \theta(0))\|$, being $\pi(\tau_k, \theta(\tau_k))$ a performance vector defined by the modulus of the closed-loop poles. The solution of the proposed problem yields

$$\Omega = -(\Delta^T W^T W \Delta)^{-1} W^T \Delta^T \lambda_{\tau_k} \quad (6)$$

where W is a weighting filter (to give priority to dominant closed-loop poles), Δ is a Jacobian matrix that includes the derivatives $\frac{\partial \pi}{\partial \theta_i}$ evaluated at the nominal point (i.e., for $\tau_k = 0$ and $\theta(0)$) for each controller parameter θ_i , and λ_{τ_k} is the derivative related to the delay, $\lambda_{\tau_k} = \frac{\partial \pi}{\partial \tau_k}$, evaluated at the same nominal point. The scheduling law in (5) tries to maintain the no-delay nominal control performance despite network delays. See [28] for more details.

B. Event-Triggered Conditions

Two different event-triggered conditions will be considered for the WNCS. The first one is related to the system's output y_k (and hence, defined at the sensor device, which is located at the

local side) and the other one to the tracking error e_k (which is defined at the remote side).

Let $\beta_k \in \{0, 1\}$ denote the scheduling variable at the sensor in the sense that $\beta_k = 1$ if the sensor data y_k is transmitted at discrete time k over the local-to-remote link, and $\beta_k = 0$ otherwise. The last sent sensor data are stored in \hat{y}_k . Therefore

$$\hat{y}_k = \beta_k y_k + (1 - \beta_k) \hat{y}_{k-1} \quad \text{for } k \in \mathbb{N}_{\geq 1} \quad (7)$$

and given $\hat{y}_0 = y_0$. Regarding the periodic event-triggered condition at the sensor, it is implemented following a discrete-time version of the so-called mixed triggered mechanism [48] based on the system output y_k in such a way that the output y_k is sent via the network to the remote side (i.e., $\beta_k = 1$) when

$$\|\hat{y}_{k-1} - y_k\|^2 \geq \sigma_s \|y_k\|^2 + \delta_s \quad \text{for } k \in \mathbb{N}_{\geq 1} \quad (8)$$

given $\hat{y}_0 = y_0$, and where σ_s and δ_s are positive constants. Note that, usually, σ_s is chosen to be smaller than 1, since for large values of σ_s , this condition would hardly be met (see, e.g., [49] and the literature therein). It is also often the case to have values of σ_s close to zero or even zero.

Let $\gamma_k \in \{0, 1\}$ denote the scheduling variable for the tracking error signal, which is evaluated at the remote side when a packet from the sensor arrives (that is, when $\beta_k = 1$; otherwise, it is not). In particular, $\gamma_k = 1$ denotes transmission of the tracking error e_k over the remote-to-local link, and $\gamma_k = 0$ otherwise. A ZOH at the input of the controller (at local side) is considered to store the last sent error \hat{e}_k

$$\hat{e}_k = \gamma_k e_k + (1 - \gamma_k) \hat{e}_{k-1} \quad \text{for } k \in \mathbb{N}_{\geq 1} \quad (9)$$

where $\hat{e}_0 = e_0$ and $e_k = r_k - y_k$ (being r_k the reference signal, and $\hat{y}_k = y_k$ since $\beta_k = 1$) is transmitted to the local side (i.e., $\gamma_k = 1$) when $\beta_k = 1$ and

$$\|\hat{e}_{k-1} - e_k\|^2 \geq \sigma_e \|e_k\|^2 + \delta_e \quad (10)$$

where σ_e and δ_e are positive constants. Similarly to the discussion pertaining the choice of σ_s , note that typically σ_e is chosen to be less than 1.

Note that the feedback loop is only closed from local to remote sides, and back to local side, when the conditions (8) and (10) hold (and hence, $\beta_k = \gamma_k = 1$). If one of the event conditions is not true (that is, $\beta_k = 0$ or $\gamma_k = 0$), then there is no update of e_k , but the controller can use the last sent error \hat{e}_k (provided by the ZOH) to evolve its dynamics, which enables to retain a satisfactory control performance.

Depending on β_k and γ_k , two different dual-rate sampling schemes will be considered (depicted in Fig. 2).

- 1) If $\beta_k = 0$ or $\gamma_k = 0$, the dual-rate controller generates U_k from the last sent error ($\hat{e}_k = \hat{e}_{k-1}$) and considers $\tau_k = 0$, and the actuator injects the set of control actions following a uniform pattern. That is the lifted framework in (1). Let us denote U_k as $\tilde{U}_k = (\hat{u}_1^k, \hat{u}_2^k, \dots, \hat{u}_N^k)^T$ in this case.
- 2) If $\beta_k = \gamma_k = 1$, and due to the network-induced delay τ_k , another value u_0^k appears in the control input sequence $\tilde{U}_k = (u_0^k, u_1^k, u_2^k, \dots, u_N^k)^T$. The value u_0^k is actually the first control action calculated from the held error, that is, $u_0^k = \hat{u}_1^k$. This computation is carried out before

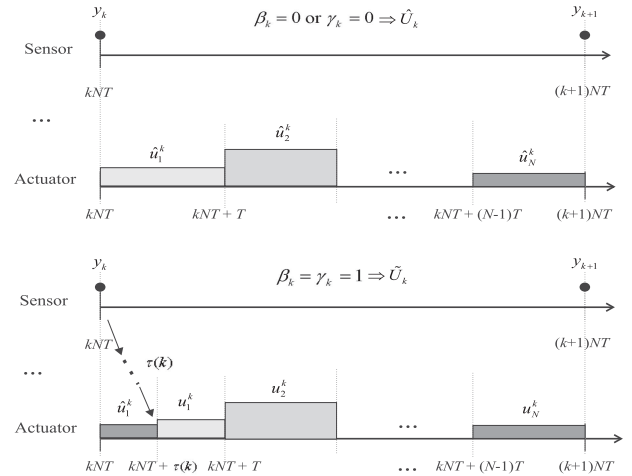


Fig. 2. Time axis for the dual-rate sampling strategy.

the updated error is received by the controller. After τ_k , the error is received, and hence, $\hat{e}_k = e_k$, and from this information, the remaining control actions of \tilde{U}_k (i.e., (u_1^k, \dots, u_N^k)) are computed, replacing those previously calculated from the outdated error (i.e., $(\hat{u}_1^k, \dots, \hat{u}_N^k)$). Therefore, in this case, if every control action is applied (that is, if $\tau_k < T$), the set of control actions \tilde{U}_k to be applied by the actuator follows the nonuniform actuation pattern $\{0, \tau_k, T, \dots, (N-1)T\}$ inside the sensor period. Otherwise, if the delay were $\tau_k \geq dT$, $d \in \mathbb{N}^+$, the first d control actions in the subset $(u_1^k, u_2^k, \dots, u_N^k)$ would not be applied.

III. STABILITY ANALYSIS AND COST FUNCTIONS

In this section, first, after presenting the closed-loop model for the considered WNCS, closed-loop stability is ensured by means of LMIs. Second, two cost functions are introduced to analyze the tradeoff between control performance and resource usage.

A. Stability Analysis

We make some simplifying assumptions to streamline the stability analysis.

First, we assume that the delay coincides with one of the actuation update times $\tau_k \in \{T, \dots, (N-1)T\}$. From an implementation point of view, this can be obtained by adding an artificial delay on the local side to enforce this condition. That is, as the local side is assumed to have computation capabilities, once the round-trip time delay is measured, simple operations can be carried out to decide what is the next actuation time. Then, from this assumption, the description given at the end of the previous section, we can conclude the following. At times at which there are two transmissions ($\beta_k = 1$ and $\gamma_k = 1$), the

controller update equations and the control input are given by

$$\begin{aligned}\phi_{k+1} &= A_R(\tau_k)\phi_k + B_R(\tau_k)e_k \\ \hat{U}_k &= C_R(0)\phi_k + D_R(0)\hat{e}_{k-1} \\ \underline{U}_k &= C_R(\tau_k)\phi_k + D_R(\tau_k)e_k \\ U_k &= \chi(\tau_k)\underline{U}_k + (I - \chi(\tau_k))\hat{U}_k\end{aligned}\quad (11)$$

where, assuming $u_j^k \in \mathbb{R}^{n_u}$ for every k and j , and defining $\chi_i(j) = 1$ if $j \leq i$ and $\chi_i(j) = 0$ otherwise

$$\chi(\tau_k) = \text{diag} \left([0I_{n_u} \quad \chi_1\left(\frac{\tau_k}{T}\right)I_{n_u} \quad \dots \quad \chi_{N-1}\left(\frac{\tau_k}{T}\right)I_{n_u}] \right)$$

and where I_{n_u} denotes the $n_u \times n_u$ identity matrix. These equations can alternatively be written as

$$\begin{aligned}\phi_{k+1} &= A_R(\tau_k)\phi_k + B_R(\tau_k)e_k \\ U_k &= \bar{C}_R(\tau_k)\phi_k + \bar{D}_R(\tau_k)e_k + \tilde{D}_R(\tau_k)\hat{e}_{k-1}\end{aligned}\quad (12)$$

where

$$\begin{aligned}\bar{C}_R(\tau_k) &= \chi(\tau_k)C_R(\tau_k) + (I - \chi(\tau_k))C_R(0) \\ \bar{D}_R(\tau_k) &= \chi(\tau_k)D_R(\tau_k) \\ \tilde{D}_R(\tau_k) &= (I - \chi(\tau_k))D_R(0).\end{aligned}$$

At times at which either $\beta_k = 0$ or $\gamma_k = 0$, we have the following:

$$\begin{aligned}\phi_{k+1} &= A_R(0)\phi_k + B_R(0)\hat{e}_{k-1} \\ U_k &= C_R(0)\phi_k + D_R(0)\hat{e}_{k-1}.\end{aligned}$$

We make the following additional assumptions to make the stability analysis simpler.

A1) Either the reference is zero at every time step (i.e., $r_k = 0$), and thus, $y_k = -e_k$, or $\sigma_s = \sigma_e = 0$, and the reference is constant.

A2) $\delta_e = \delta_s$, $\sigma_s = \sigma_e$.

Due to (A1) and (A2), the triggering conditions (8) and (10) are equivalent (i.e., $\beta_k = \gamma_k$ for every $k \in \mathbb{N}$), and we can consider just one of the conditions. Let

$$v_k = y_k - \hat{y}_{k-1}$$

and

$$\xi_k = \begin{bmatrix} x_k \\ \phi_k \\ v_k \end{bmatrix}.$$

Note that

$$\hat{y}_k = \begin{cases} C_P x_k - v_k, & \text{if } \beta_k = 0 \\ C_P x_k, & \text{if } \beta_k = 1 \end{cases}.$$

Taking into account these equations and the assumptions mentioned above, we can write the closed-loop system as

$$\xi_{k+1} = \begin{cases} F_0 \xi_k, & \text{if } \xi_k^\top Q_0 \xi_k < \delta_e \\ F_1(\tau_k) \xi_k, & \text{if } \xi_k^\top Q_0 \xi_k \geq \delta_e \end{cases}\quad (13)$$

where F_1 and F_0 are defined in (15) as shown at the bottom of this page

$$Q_0 = \begin{bmatrix} -\sigma_e C_P^\top C_P & 0 & 0 \\ 0 & 0 & 0 \\ 0 & 0 & I \end{bmatrix}.\quad (14)$$

If $\delta_e = \delta_s = 0$, we can consider a common Lyapunov function and use the S-procedure to prove that $\mathbb{E}[\xi_k^\top \xi_k] \rightarrow 0$ as $k \rightarrow \infty$ if the LMIs

$$\begin{aligned}F_0^\top P F_0 - P - \zeta_1 Q_0 &< 0 \\ \mathbb{E}_\tau[F_1(\tau)^\top P F_1(\tau)] - P + \zeta_2 Q_0 &< 0\end{aligned}\quad (16)$$

hold, where τ denotes, and will denote in the following, a dummy variable with the same distribution as each τ_k , for some $\zeta_1 \geq 0$ and $\zeta_2 \geq 0$, which can be found by gridding the parameter space (similar arguments can be found in [50]).

Interestingly, considering $\delta_e = \delta_s > 0$, one can still establish a stability property, commonly known as mean square stability, by testing the LMIs (16), as the next result shows.

Theorem 1: Suppose that the LMIs (16) hold for some $\zeta_1 \geq 0$ and $\zeta_2 \geq 0$. Then, there exists $c > 0$, dependent on the initial condition ξ_0 , such that the following holds for the system (13):

$$\mathbb{E}[\xi_k^\top \xi_k] \leq c\quad (17)$$

for every $k \in \mathbb{N}$.

Proof: We start by establishing that the LMIs (16) imply that there exist $d > 0$ and $\alpha < 1$ such that

$$\mathbb{E}[\xi_{k+1}^\top P \xi_{k+1} | \xi_k] - \alpha \xi_k^\top P \xi_k < d, \quad \text{for every } \xi_k.\quad (18)$$

Using the S-Procedure, we can conclude that (18) holds for ξ_k such that $\xi_k^\top Q_0 \xi_k \geq \delta_e$, if there exists $\zeta_3 \geq 0$ such that

$$\mathbb{E}[\xi_{k+1}^\top P \xi_{k+1} | \xi_k] - \alpha \xi_k^\top P \xi_k - d + \zeta_3 (\xi_k^\top Q_0 \xi_k - \delta_e) < 0$$

$$\begin{aligned}F_0 &= \begin{bmatrix} A_P - B_P D_R(0) C_P & B_P C_R(0) & B_P D_R(0) \\ -B_R(0) C_P & A_R(0) & B_R(0) \\ C_P (A_P - B_P D_R(0) C_P) - C_P & C_P B_P C_R(0) & C_P B_P D_R(0) + I \end{bmatrix} \\ F_1(\tau_k) &= \begin{bmatrix} A_P - B_P (\tilde{D}_R(\tau_k) + \bar{D}_R(\tau_k)) C_P & B_P \bar{C}_R(\tau_k) & B_P \tilde{D}_R(\tau_k) \\ -B_R(\tau_k) C_P & A_R(\tau_k) & 0 \\ C_P (A_P - B_P (\tilde{D}_R(\tau_k) + \bar{D}_R(\tau_k)) C_P) - C_P & C_P B_P \bar{C}_R(\tau_k) & C_P B_P \tilde{D}_R(\tau_k) \end{bmatrix}\end{aligned}\quad (15)$$

for every ξ_k or equivalently

$$\begin{aligned} & \xi_k^\top (\mathbb{E}[F_1(\tau_k)^\top P F_1(\tau_k)] - P + \zeta_3 Q_0) \xi_k - \\ & - \zeta_3 \delta_e - d + (1 - \alpha) \xi_k^\top P \xi_k < 0. \end{aligned} \quad (19)$$

Making $\zeta_3 = \zeta_1$, and noticing that from the second inequality in (16), $\mathbb{E}_\tau[F_1(\tau)^\top P F_1(\tau)] - P + \zeta_3 Q_0 = -S_1$ for some $S_1 > 0$, choosing $0 < \alpha < 1$ such that $(1 - \alpha)P - S_1 < 0$, we conclude that (19) holds.

Using again the S-Procedure, we can conclude that (18) holds for ξ_k such that $\xi_k^\top Q_0 \xi_k < \delta_e$, if there exists $\zeta_4 \geq 0$ such that

$$\mathbb{E}[\xi_{k+1}^\top P \xi_{k+1} | \xi_k] - \alpha \xi_k^\top P \xi_k - d - \zeta_4 (\xi_k^\top Q_0 \xi_k - \delta_e) < 0$$

or equivalently

$$\xi_k^\top [F_0^\top P F_0 - P - \zeta_4 Q_0] \xi_k - (d - \zeta_4 \delta_e) + (1 - \alpha) \xi_k^\top P \xi_k < 0. \quad (20)$$

Making $\zeta_4 = \zeta_1$, noticing that from the first inequality in (16), $F_0^\top P F_0 - P - \zeta_4 Q_0 = -R_1$ for some $R_1 > 0$, choosing $0 < \alpha < 1$ such that $(1 - \alpha)P - R_1 < 0$, and picking $d > \zeta_4 \delta_e$, we conclude that the inequality (20) holds, which concludes the proof of (18).

Applying recursively (18) and using the tower property of conditional expectations, we conclude that, for $k \geq 0$,

$$\mathbb{E}[\xi_{k+1}^\top P \xi_{k+1}] < \alpha \xi_0^\top P \xi_0 + \sum_{\ell=0}^k \alpha^\ell d, \quad \text{for every } \xi_k \quad (21)$$

which implies (17) due to the fact that P is positive definite. ■

Discussion on feasibility of the LMIs: The LMI

$$\mathbb{E}_\tau[F_1(\tau)^\top P F_1(\tau)] - P + \zeta_2 Q_1 < 0$$

should be feasible even for $\zeta_2 = 0$, since this corresponds to a situation where there is a transmission. The feasibility of this LMI can alternatively be tested by checking if the following matrix:

$$L = \mathbb{E}_\tau[F_1(\tau)^\top \otimes F_1(\tau)^\top] \quad (22)$$

is Schur stable, where \otimes is the Kronecker product (see [51]).

Note that

$$F_0^\top P F_0 - P < 0$$

would never hold if the plant is open-loop unstable.

However, as the next lemma shows, the first inequality in (16) is always satisfied when $\sigma_e = \sigma_s = 0$, and the controller stabilizes the plant if one would have $\hat{e}_k = e_k$, i.e.,

$$\phi_{k+1} = A_R(0)\phi_k + B_R(0)e_k$$

$$U_k = C_R(0)\phi_k + D_R(0)e_k$$

which can be easily shown to be equivalent to the following matrix:

$$M := \begin{bmatrix} A_P - B_P D_R(0) C_P & B_P C_R(0) \\ -B_R(0) C_P & A_R(0) \end{bmatrix} \quad (23)$$

being Schur stable.

Lemma 1: Suppose that $\sigma_s = \sigma_e = 0$ and that M is Schur stable. Then, there exists (a sufficiently large) $\zeta_1 > 0$ such that the LMI

$$F_0^\top P F_0 - P - \zeta_1 Q_0 < 0$$

is feasible.

Proof: Note that, due the assumption that M is Schur stable, there exists a positive definite P_{cl} such that

$$M^\top P_{cl} M - P_{cl} = -R_{cl} < 0$$

for some positive definite R_{cl} (which can be picked arbitrarily). Moreover

$$F_0 = \begin{bmatrix} M & N \\ R & Q \end{bmatrix}$$

where M is defined above, and the expressions for N , R , and Q can be easily obtained. Suppose that we pick P taking the form

$$P = \begin{bmatrix} P_{cl} & 0 \\ 0 & P_e \end{bmatrix}$$

for positive definite P_{cl} and P_e . Then, using the fact that $\sigma_s = \sigma_e = 0$,

$$F_0^\top P F_0 - P - \zeta_1 Q_0 = \begin{bmatrix} -R_{cl} & S_1 \\ S_1^\top & R_1 - \zeta_1 I \end{bmatrix}$$

for some matrices S_1 and R_1 , whose expressions are omitted. By considering a sufficiently large ζ_1 , one can prove that the latter matrix is negative definite, concluding the proof. ■

B. Cost Functions About Control Performance and Resource Utilization

In order to compare the proposed PETS-based control solution with the conventional TTS one, control performance and resource utilization may be evaluated. For this purpose, two different cost functions are proposed.

- 1) J_1 , which is based on the ℓ_2 -norm, and its goal is to provide a measure about how accurate the reference r_k is followed along m iterations:

$$J_1 = \sqrt{\sum_{k=1}^m e_k^2}. \quad (24)$$

- 2) J_2 : In order to analyze the network usage in the PETS strategy (which may be related to the battery usage of the different devices when sending packets through the network), let us define the number of transmitted packets as NoT_{PETS} , which will be compared with the number of transmissions carried out in the TTS approach NoT_{TTS} . In this way, the network usage J_2 (in percent) can be expressed for the PETS strategy as

$$J_2 = \frac{NoT_{PETS}}{NoT_{TTS}} \cdot 100\%. \quad (25)$$

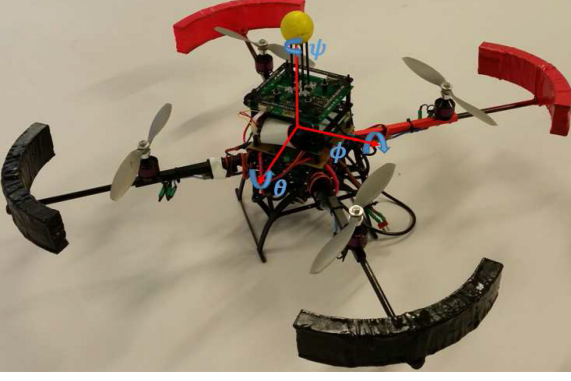


Fig. 3. Four-rotor UAV.

IV. APPLICATION TO A UAV-BASED TEST-BED PLATFORM

In this section, the proposed WNCS is simulated and experimentally validated considering a UAV as the process to be controlled. The main goal of this section is to present the main benefits of the PETS-based strategy compared to the TTS-based one, regarding the tradeoff between network utilization and control performance (see Section III-B for the performance measures). The section is split into four parts. First, the experimental platform in which the control solution is implemented is briefly described. From this description, important data used for the simulation will be obtained (transfer function, delay distribution, control parameters, and so on). Second, the stability conditions presented in Section III-A will be checked in order to prove stability for the proposed WNCS. Third, by means of a Truetime application [42], the cost functions exposed in Section III-B will be evaluated. Finally, the control solution is implemented in the test-bed platform, and experimental validations are provided (also computing the cost functions in Section III-B).

A. Description of the Test-Bed Platform

The proposed WNCS considers a four-rotor UAV as the process to be controlled, which is commonly called as quadrotor (see Fig. 3). This platform can be seen as a rigid body with no constraints, having six degrees of freedom, being three position coordinates (x, y, z) , and three Euler angles (ϕ, θ, ψ) (which, respectively, represent pitch, roll, and yaw). The platform is connected to a GCS via WiFi, which works as the remote device in Fig. 1.

Using the four rotors as actuators, the six variables can be controlled. Due to the intrinsic instability of the system, in this platform, an onboard control for the roll and pitch angles is already implemented in order to get autostabilization. In this application, the orientation along z , i.e., the yaw angle ψ , will be controlled. This angle can be approximately modeled by means of the following transfer function:

$$G(s) = \frac{\psi(s)}{u(s)} = \frac{1175}{s^2} \quad (26)$$

where $u(s)$ is a virtual control action related to the rotor's speed, which will be saturated in the range $[-0.2, 0.2]$.

A histogram of the round-trip time delays $\tau(k)$ measured in the WNCS is depicted in Fig. 4. As the maximum delay τ_{\max} is

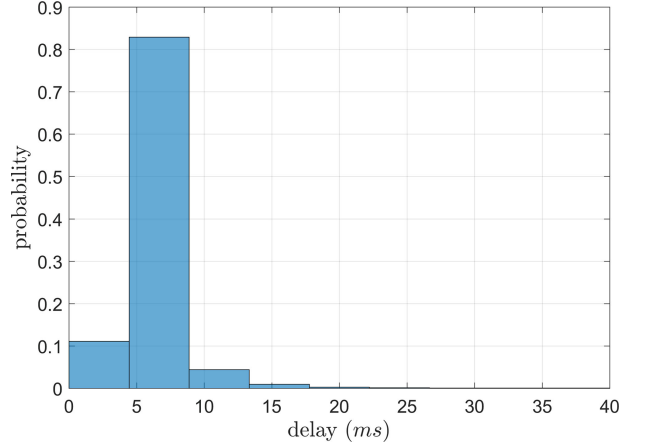


Fig. 4. Experimental round-trip time delay $\tau(k)$.

less than 40 ms, the sensor period is chosen as $NT = 40$ ms in order to ensure no packet disorder. In addition, since most of the delays τ_k are less than 20 ms, N can be defined as $N = 2$, being $T = 20$ ms. As the situation in which $\tau_k < T$ is often given, when $\beta_k = \gamma_k = 1$ (bottom subplot in Fig. 2), the N control actions will be in most of the cases applied.

The TTS strategy defines the desired control performance for ψ . In this application, we use the following control requirements to design the nominal controller: settling time $t_s \leq 1.5$ s and overshoot $\delta \leq 15\%$. Then, the nominal parameters of the dual-rate controller are $\theta(0) = (K_p(0), K_d(0), f(0))^T = (0.023, 0.45, 0.15)^T$. To face the network-induced delays, the scheduling vector in (6) is $\Omega = (K_p, K_d, f)^T = (-0.10038, -375.4386, 0.8614)^T$. When using a PETS context, first, the values to be considered for the thresholds in (8) and (10) will be $\sigma_s = \sigma_e = 0$ and $\delta_s = \delta_e = 0.125$. In this way, the two assumptions needed to assess stability in Section III-A are fulfilled. Second, a different, more flexible configuration for the thresholds will be tested, where $\sigma_s = 0.3125$, $\sigma_e = 0.03125$, $\delta_s = 0.125$, and $\delta_e = 0.0125$.

B. Stability Check

From the first PETS case, $\sigma_s = \sigma_e = 0$; then, we can simply resort to Lemma 1 to assert the feasibility of the first LMI in (16). Computing the eigenvalues of M in (23) and L in (22), we conclude that both of them are Schur matrices, and therefore, mean square stability is guaranteed (and, in addition, the LMIs in (16) are satisfied).

C. Truetime Simulation

The simulation application is developed in Truetime [42], considering a wireless local area network. The study will compare both approaches: TTS versus PETS. First, the results obtained by the TTS strategy are depicted in Fig. 5. At the top subplot, output ψ and reference r can be observed. The index J_1 is calculated from this subplot (Table I shows the consequent value). At the bottom subplot, a binary variable shows the network usage, that is, 0 means that the network is not being used, and 1 means that the network is being used. In this case,

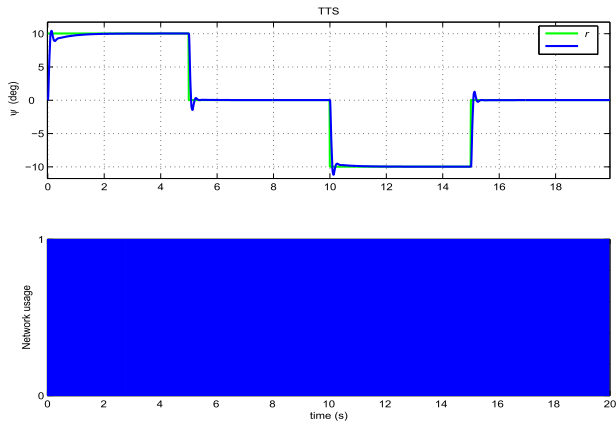


Fig. 5. System behavior for the TTS strategy. Simulation.

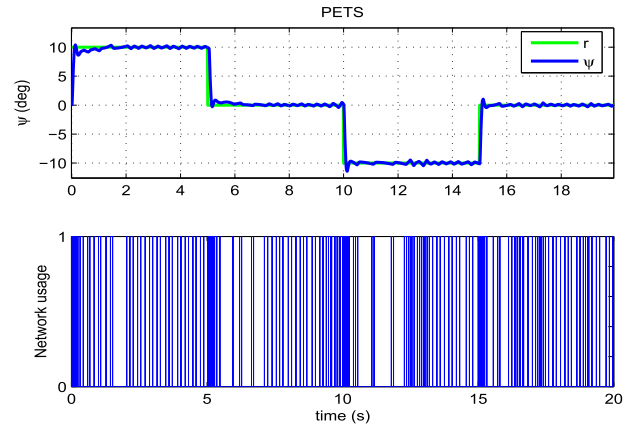


Fig. 7. System behavior for the PETS strategy (case 2). Simulation.

TABLE I
 J_1 AND J_2 INDEXES FOR THE SIMULATION

index	TTS	PETS (case 1)	PETS (case 2)
J_1	101.16	107.86	105.20
J_2	100	26.74	32.13

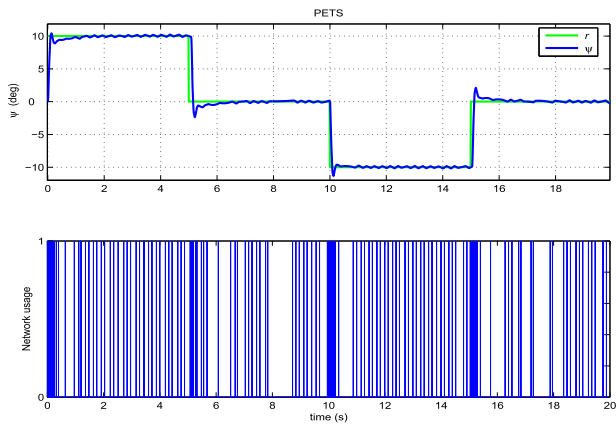


Fig. 6. System behavior for the PETS strategy (case 1). Simulation.

the network is completely used (at every period NT), and hence, $J_2 = 100\%$.

Second, Figs. 6 and 7 show the results obtained by the PETS strategy. As shown in the top subplot, the dynamic control specifications (t_s, δ) are generally reached, but some worsening in the steady-state response is observed. This fact is verified when computing J_1 . In the first PETS case, this cost function is increased around 7% compared to the TTS case. In the second PETS case, it is increased around 4% (see Table I). In both PETS cases, the bottom subplot shows a clear reduction of the network usage compared to the TTS strategy, which is quantified by means of a decrease of around 73% in J_2 for the first case and 67% for the second case (as shown in Table I). The conclusion of these results is that the second PETS case achieves a 3% more accurate reference tracking, but consuming 6% more resources. The differences between both cases can be considered to be not very significant. Therefore, and since network usage is more reduced in the first PETS case, we will only use this instance in the experimental validation.

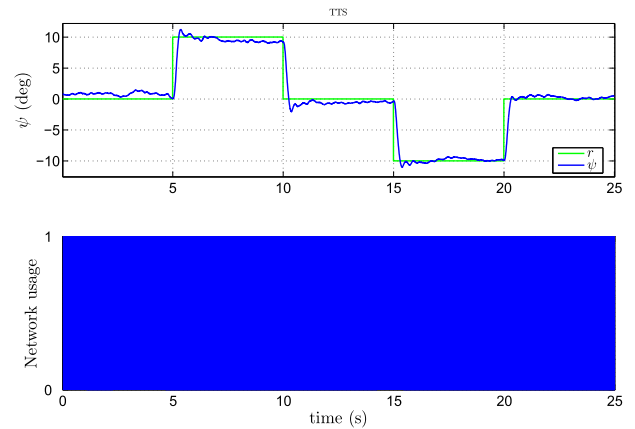


Fig. 8. System behavior for the TTS strategy. Experiment.

TABLE II
 J_1 AND J_2 INDEXES FOR THE EXPERIMENT

index	TTS	PETS
J_1	120.77	135.02
J_2	100	24.37

D. Validation on the Test-Bed Platform

Now, real experiments are carried out with the quadcopter, validating the previous results. First, the results obtained on the experimental platform by the TTS strategy are depicted in Fig. 8. Table II presents the results for the indexes J_1 and J_2 .

Second, Fig. 9 shows the results obtained by the PETS strategy (case 1). As in the simulation, the top subplot shows that the dynamic control specifications (t_s, δ) are mostly reached, but some worsening in the steady-state response is observed. Then, J_1 is increased around 11% compared to the TTS case (see Table II). The bottom subplot shows a significant reduction of the network usage compared to the TTS strategy, as observed in the simulation. Concretely, J_2 shows a decrease of around 76% (see Table II).

Therefore, as similar values for the cost indexes and a same trend are obtained, the control solution is validated in practice, showing the potential of the proposed PETS strategy.

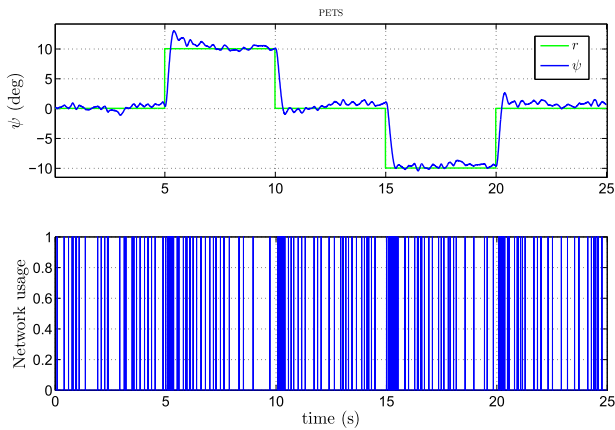


Fig. 9. System behavior for the PETS strategy (case 1). Experiment.

V. CONCLUSION

In this paper, we studied the design and experimental validation of an undegraded PETS strategy in a WNCS framework (concretely, on a UAV-based test-bed platform). Dual-rate control techniques were used to face time-varying delays and packet disorder, and to try to maintain control performance at the desired level. Integrating PETS in the WNCS enabled significant reduction of resource usage. Control system stability for the WNCS was ensured via LMIs.

One of the research directions we would like to pursue in the future is the extension of the results to nonlinear systems. Related work on PETS for nonlinear systems can be found in [11]–[14] and literature therein.

REFERENCES

- [1] P. Tabuada, "Event-triggered real-time scheduling of stabilizing control tasks," *IEEE Trans. Autom. Control*, vol. 52, no. 9, pp. 1680–1685, Sep. 2007.
- [2] K. J. Aström, "Event based control," in *Analysis and Design of Nonlinear Control Systems*. New York, NY, USA: Springer, 2008, pp. 127–147.
- [3] W. Heemels, J. Sandee, and P. Van Den Bosch, "Analysis of event-driven controllers for linear systems," *Int. J. Control*, vol. 81, no. 4, pp. 571–590, 2008.
- [4] W. Heemels and M. Donkers, "Model-based periodic event-triggered control for linear systems," *Automatica*, vol. 49, no. 3, pp. 698–711, 2013.
- [5] J. Lunze and D. Lehmann, "A state-feedback approach to event-based control," *Automatica*, vol. 46, no. 1, pp. 211–215, 2010.
- [6] X. Chen and F. Hao, "Periodic event-triggered state-feedback and output-feedback control for linear systems," *Int. J. Control, Autom. Syst.*, vol. 13, no. 4, pp. 779–787, 2015.
- [7] W. Heemels, G. Dullerud, and A. Teel, "L₂-gain analysis for a class of hybrid systems with applications to reset and event-triggered control: A lifting approach," *IEEE Trans. Autom. Control*, vol. 61, pp. 2766–2781, Oct. 2016.
- [8] E. Aranda-Escolástico, C. Rodríguez, M. Guinaldo, J. L. Guzmán, and S. Dormido, "Asynchronous periodic event-triggered control with dynamical controllers," *J. Franklin Inst.*, vol. 355, pp. 3455–3469, 2018.
- [9] A. Selivanov and E. Fridman, "Event-triggered H_∞ control: A switching approach," *IEEE Trans. Autom. Control*, vol. 61, no. 10, pp. 3221–3226, Oct. 2016.
- [10] M. Braksmayer and L. Mirkin, "Redesign of stabilizing discrete-time controllers to accommodate intermittent sampling," *IFAC-PapersOnLine*, vol. 50, no. 1, pp. 2633–2638, 2017.
- [11] R. Postoyan, A. Anta, W. Heemels, P. Tabuada, and D. Nesic, "Periodic event-triggered control for nonlinear systems," in *Proc. IEEE Conf. Decis. Control*, 2013, pp. 7397–7402.
- [12] W. Wang, R. Postoyan, D. Nešić, and W. M. H. Heemels, "Stabilization of nonlinear systems using state-feedback periodic event-triggered controllers," in *Proc. IEEE 55th Conf. Decis. Control*, 2016, pp. 6808–6813.
- [13] E. Aranda-Escolástico, M. Abdelrahim, M. Guinaldo, S. Dormido, and W. Heemels, "Design of periodic event-triggered control for polynomial systems: A delay system approach," *IFAC-PapersOnLine*, vol. 50, no. 1, pp. 7887–7892, 2017.
- [14] L. Etienne, S. Di Gennaro, and J.-P. Barbot, "Periodic event-triggered observation and control for nonlinear Lipschitz systems using impulsive observers," *Int. J. Robust Nonlinear Control*, vol. 27, no. 18, pp. 4363–4380, 2017.
- [15] W. Heemels, M. Donkers, and A. R. Teel, "Periodic event-triggered control for linear systems," *IEEE Trans. Autom. Control*, vol. 58, no. 4, pp. 847–861, Apr. 2013.
- [16] A. Eqtami, D. V. Dimarogonas, and K. J. Kyriakopoulos, "Event-triggered control for discrete-time systems," in *Proc. Amer. Control Conf.*, 2010, pp. 4719–4724.
- [17] D. Li, S. Shah, and T. Chen, "Analysis of dual-rate inferential control systems," *Automatica*, vol. 38, no. 6, pp. 1053–1059, 2002.
- [18] J. Salt, Á. Cuenca, F. Palau, and S. Dormido, "A multirate control strategy to the slow sensors problem: An interactive simulation tool for controller assisted design," *Sensors*, vol. 14, no. 3, pp. 4086–4110, 2014.
- [19] J. Qiu, H. Gao, and M.-Y. Chow, "Networked control and industrial applications," *IEEE Trans. Ind. Electron.*, vol. 63, no. 2, pp. 1203–1206, Feb. 2016.
- [20] X.-M. Zhang, Q.-L. Han, and X. Yu, "Survey on recent advances in networked control systems," *IEEE Trans. Ind. Inform.*, vol. 12, no. 5, pp. 1740–1752, Oct. 2016.
- [21] L. Zhang, H. Gao, and O. Kaynak, "Network-induced constraints in networked control systems: A survey," *IEEE Trans. Ind. Inform.*, vol. 9, no. 1, pp. 403–416, Feb. 2013.
- [22] X. Luan, P. Shi, and C.-L. Liu, "Stabilization of networked control systems with random delays," *IEEE Trans. Ind. Electron.*, vol. 58, no. 9, pp. 4323–4330, Sep. 2011.
- [23] H. Li and Y. Shi, "Network-based predictive control for constrained nonlinear systems with two-channel packet dropouts," *IEEE Trans. Ind. Electron.*, vol. 61, no. 3, pp. 1574–1582, Mar. 2014.
- [24] A. Cuenca, P. García, P. Albertos, and J. Salt, "A non-uniform predictor-observer for a networked control system," *Int. J. Control, Autom. Syst.*, vol. 9, no. 6, pp. 1194–1202, 2011.
- [25] A. Liu, W.-A. Zhang, B. Chen, and L. Yu, "Networked filtering with Markov transmission delays and packet disordering," *IET Control Theory Appl.*, vol. 12, no. 5, pp. 687–693, 2018.
- [26] R. E. Julio and G. S. Bastos, "A ROS package for dynamic bandwidth management in multi-robot systems," in *Robot Operating System*. New York, NY, USA: Springer, 2017, pp. 309–341.
- [27] V. Casanova, J. Salt, A. Cuenca, and R. Piza, "Networked control systems: Control structures with bandwidth limitations," *Int. J. Syst., Control Commun.*, vol. 1, no. 3, pp. 267–296, 2009.
- [28] A. Sala, Á. Cuenca, and J. Salt, "A retunable PID multi-rate controller for a networked control system," *Inf. Sci.*, vol. 179, no. 14, pp. 2390–2402, 2009.
- [29] S. Boyd, L. El Ghaoui, E. Feron, and V. Balakrishnan, *Linear Matrix Inequalities in System and Control Theory*. Philadelphia, PA, USA: SIAM, 1994.
- [30] R. Lozano, *Unmanned Aerial Vehicles: Embedded Control*. Hoboken, NJ, USA: Wiley, 2013.
- [31] F. Kendoul, "Survey of advances in guidance, navigation, and control of unmanned rotorcraft systems," *J. Field Robot.*, vol. 29, no. 2, pp. 315–378, 2012.
- [32] R. Mahony, V. Kumar, and P. Corke, "Multirotor aerial vehicles: Modeling, estimation, and control of quadrotor," *IEEE Robot. Autom. Mag.*, vol. 19, no. 3, pp. 20–32, Sep. 2012.
- [33] Z. He and L. Zhao, "A simple attitude control of quadrotor helicopter based on Ziegler-Nichols rules for tuning PD parameters," *The Sci. World J.*, vol. 2014, 2014, Art. no. 280180.
- [34] S. Khatoun *et al.*, "Dynamic modeling and stabilization of quadrotor using PID controller," in *Proc. Int. Conf. Adv. Comput., Commun. Inform.*, 2014, pp. 746–750.
- [35] B. Zhao, B. Xian, Y. Zhang, and X. Zhang, "Nonlinear robust adaptive tracking control of a quadrotor UAV via immersion and invariance methodology," *IEEE Trans. Ind. Electron.*, vol. 62, no. 5, pp. 2891–2902, May 2015.
- [36] H. Liu, D. Li, Z. Zuo, and Y. Zhong, "Robust three-loop trajectory tracking control for quadrotors with multiple uncertainties," *IEEE Trans. Ind. Electron.*, vol. 63, no. 4, pp. 2263–2274, Apr. 2016.
- [37] R. Sanz, P. García, Q.-C. Zhong, and P. Albertos, "Robust control of quadrotors based on an uncertainty and disturbance estimator," *J. Dyn. Syst., Meas. Control*, vol. 138, no. 7, 2016, Art. no. 71006.

- [38] V. S. Dolk, J. Ploeg, and W. M. H. Heemels, "Event-triggered control for string-stable vehicle platooning," *IEEE Trans. Intell. Transp. Syst.*, vol. 18, no. 12, pp. 3486–3500, Dec. 2017.
- [39] B. A. Khashoeei, B. van Eekelen, D. Antunes, and W. Heemels, "Sub-optimal event-triggered control over unreliable communication links with experimental validation," in *Proc. Int. Conf. Event-Based Control, Commun. Signal Process.*, 2017, pp. 1–6.
- [40] G. A. Kiener, D. Lehmann, and K. H. Johansson, "Actuator saturation and anti-windup compensation in event-triggered control," *Discrete Event Dyn. Syst.*, vol. 24, no. 2, pp. 173–197, 2014.
- [41] J. Araújo, M. Mazo, A. Anta, P. Tabuada, and K. H. Johansson, "System architectures, protocols and algorithms for aperiodic wireless control systems," *IEEE Trans. Ind. Inform.*, vol. 10, no. 1, pp. 175–184, Feb. 2014.
- [42] A. Cervin, D. Henriksson, B. Lincoln, J. Eker, and K.-E. Arzén, "How does control timing affect performance? Analysis and simulation of timing using Jitterbug and TrueTime," *IEEE Control Syst. Mag.*, vol. 23, no. 3, pp. 16–30, Jun. 2003.
- [43] P. Khargonekar, K. Poolla, and A. Tannenbaum, "Robust control of linear time-invariant plants using periodic compensation," *IEEE Trans. Autom. Control*, vol. AC-30, no. 11, pp. 1088–1096, Nov. 1985.
- [44] T. Cooklev, J. C. Eidson, and A. Pakdaman, "An implementation of IEEE 1588 over IEEE 802.11b for synchronization of wireless local area network nodes," *IEEE Trans. Instrum. Meas.*, vol. 56, no. 5, pp. 1632–1639, Oct. 2007.
- [45] Y. Tipsuwan and M. Chow, "Gain scheduler middleware: A methodology to enable existing controllers for networked control and teleoperation—Part I: networked control," *IEEE Trans. Ind. Electron.*, vol. 51, no. 6, pp. 1218–1227, Dec. 2004.
- [46] K. Ogata, *Discrete-time Control Systems*, vol. 2. Englewood Cliffs, NJ, USA: Prentice-Hall, 1995.
- [47] K. J. Åström and T. Häggglund, *PID Controllers: Theory, Design, and Tuning*, vol. 2. Research Triangle Park, NC, USA: Instrum. Soc. Amer., 1995.
- [48] D. P. Borgers and W. M. H. Heemels, "Event-separation properties of event-triggered control systems," *IEEE Trans. Autom. Control*, vol. 59, no. 10, pp. 2644–2656, Oct. 2014.
- [49] L. Xing, C. Wen, Z. Liu, H. Su, and J. Cai, "Event-triggered adaptive control for a class of uncertain nonlinear systems," *IEEE Trans. Autom. Control*, vol. 62, no. 4, pp. 2071–2076, Apr. 2017.
- [50] D. Antunes, J. P. Hespanha, and C. Silvestre, "Stochastic networked control systems with dynamic protocols," *Asian J. Control*, vol. 17, no. 1, pp. 99–110, 2015.
- [51] O. Costa, M. Fragoso, and R. Marques, *Discrete-Time Markov Jump Linear Systems*. New York, NY, USA: Springer, 2005.



Ángel Cuenca received the M.Sc. degree in computer science and the Ph.D. degree in control engineering from the Technical University of Valencia (UPV), Valencia, Spain, in 1998 and 2004, respectively.

He is currently an Associate Professor with the Systems Engineering and Control Department, UPV. He was a Visiting Scholar at the Lund Institute of Technology, Lund, Sweden, in 2008, with the North Carolina State University, Raleigh, NC, USA, in 2012, with the Eindhoven

University of Technology, Eindhoven, The Netherlands, in 2014, and with the University of California, Berkeley, CA, USA, in 2016 and 2018. His research interests include networked and event-triggered control systems, and multirate control systems.



Duarte J. Antunes (M'11) was born in Viseu, Portugal, in 1982. He received the Licenciatura degree in electrical and computer engineering from the Instituto Superior Técnico (IST), Lisbon, Portugal, in 2005, and the Ph.D. degree in automatic control from the Institute for Systems and Robotics, IST, in 2011.

From 2011 to 2013, he was a Postdoctoral Researcher with the Eindhoven University of Technology, Eindhoven, The Netherlands, where he is currently an Assistant Professor with the Department of Mechanical Engineering. His research interests include networked control systems, stochastic control, approximate dynamic programming, and robotics.



Alberto Castillo (S'17) was born in Valencia, Spain, in 1992. He received the B.Sc. degree in industrial engineering and M.Sc. degree in industrial engineering with a major in process control from the School of Industrial Engineers, Technical University of Valencia (UPV), Valencia, Spain, in 2013 and 2016, respectively.

He has been with the Department of Systems Engineering and Control, UPV, since 2014. He was a Research Collaborator at the Institute of Cyber-Systems and Control, Zhejiang University, Hangzhou, China. His current research interests include disturbance rejection-based control theory and quadrotor control algorithms.

Mr. Castillo was a recipient of the Ph.D. fellowship, FPU15/02008, in 2016.



Pedro García was born in Requena, Spain. He received the Ph.D. degree in control systems and industrial computing from the Technical University of Valencia (UPV), Valencia, Spain, in 2007.

He is currently an Associate Professor of automatic control with UPV. He was a Visiting Researcher at the Lund Institute of Technology, Lund, Sweden, with the Université de Technologie de Compiègne, France, with the University of Florianópolis, Brazil, with the University of Sheffield, U.K., and with Zhejiang University, Hangzhou, China. He has coauthored one book and more than 70 refereed journal and conference papers. His current research interests include control of time-delay systems, predictive control, disturbance observers, real-time applications, and unmanned aerial vehicles.



Behnam Asadi Khashoeei received the M.Sc. degree (*cum laude*) in electrical engineering from the Isfahan University of Technology, Isfahan, Iran, in 2012, and the Ph.D. degree in mechanical engineering from the Eindhoven University of Technology, Eindhoven, The Netherlands, in 2017.

His research interests include optimal control theory, networked control systems, and event-triggered control.



W. P. M. H. Heemels (F'06) received the M.Sc. degree in mathematics and the Ph.D. degree in control theory (both *summa cum laude*) from the Eindhoven University of Technology (TU/e), Eindhoven, The Netherlands, in 1995 and 1999, respectively.

From 2000 to 2004, he was with the Department of Electrical Engineering Department, TU/e, and from 2004 to 2006 with the Embedded Systems Institute (ESI). Since 2006, he has been with the Department of Mechanical Engineering, TU/e, where he is currently a Full Professor. He was a Visiting Professor at the Swiss Federal Institute of Technology, Switzerland, in 2001, and with the University of California at Santa Barbara in 2008. In 2004, he was with the company Océ, Venlo, The Netherlands. His current research interests include hybrid and cyber-physical systems, networked and event-triggered control systems, and constrained systems including model-predictive control.

Dr. Heemels served/serves on the Editorial Boards of *Automatica*, *Nonlinear Analysis: Hybrid Systems*, the *Annual Reviews in Control*, and the IEEE TRANSACTIONS ON AUTOMATIC CONTROL. He was a recipient of a personal VICI grant awarded by the Dutch Technology Foundation.